Crosby, G. A.; Kata, M. *J. Am. Chem. Soc.* **1977**, *99*, 278.
(11) Rabinowitz, R.; Marcus, R.; Pellon, J. *J. Polym. Sci., Part A* **1964**, *2*, 1241.
(12) These estimates are at best oversimplified since sequence calculations are based on homogeneous polymerizations while in the present example the cross-linked polymer is precipitated as it forms.
(13) Rabinowitz, R.; Marcus, R. *J. Org. Chem.* **1971**, *26*, 4157.

Communications to the Editor

The QELS "Slow Mode" Is a Sample-Dependent Phenomenon in Poly(methyl methacrylate) Solutions

Recent studies of the spectrum of light scattered from semidilute polymer solutions have attempted to characterize and interpret the two observed relaxation modes.[1-11] The fast relaxation has been established as being characteristic of cooperative or mutual diffusion,[12] but the origin of the slow mode is as yet unexplained. Early studies concluded that the slow mode was representative of polymer self-diffusion.[4-6,10] However, discrepancies between apparent diffusion rates from the slow mode and self-diffusion data from other techniques called this conclusion into question.[7,9] In particular, the magnitude of the slow-mode diffusion data is consistently 1 or 2 orders of magnitude lower than that of the self-diffusion data. Most recently, the formation of transient entangled macromolecular clusters has been proposed as the physical mechanism responsible for the slow-mode relaxation.[9,11] We report here the results of a comprehensive light scattering study of nine poly(methyl methacrylate) samples in solutions in methyl methacrylate. The existence of the slow mode is found to be sample dependent and not an intrinsic property of semidilute polymer solutions. Furthermore, evidence is presented to support the transient cluster hypothesis as the mechanism responsible for the slow mode in solutions where we observe it.

Experimental Section. The properties and sources of the PMMA samples studied are given in Table I. Each polymer sample was dissolved in methyl methacrylate (Aldrich Chemical Co.) to a concentration of 0.100 g/mL. Light scattering cells were rinsed repeatedly with filtered solvent to eliminate dust. The 0.100 g/mL solutions were filtered through 0.2-μm Rainin nylon filters into the clean cells. Less concentrated samples were prepared by dilution with filtered solvent. Samples of higher concentration were prepared by fitting the scattering cell with a 0.45-μm Rainin filter unit as a lid, which allowed for MMA evaporation under dust-free conditions. All concentrations were determined by weighing, and all sample cells were sealed after preparation.

An identical procedure was used to prepare sample solutions of one of the PMMA samples in chloroform.

Dynamic light scattering experiments were carried out on a Malvern Type PCS-100M spectrometer using a Lexel Model 95-2 argon ion laser and a Langley-Ford Model 1096 correlator. Total intensity light scattering measurements were made on a Sofica apparatus.

Results and Discussion. The autocorrelation functions obtained for dilute solutions of the PC and PL samples were well represented by single exponentials. Dilute solutions of the more polydisperse PI, D, and FR samples showed a broader distribution of diffusive relaxation times as determined by analysis using the CONTIN program of Provencher.[13] For all samples studied, the distribution of relaxation times in dilute solution was unimodal. At higher concentrations, however, discrepancies in the scattering behavior among the different PMMA samples were observed. The PI, PL, D, and FR samples exhibited unimodal relaxation time distributions up to the highest concentrations studied. In contrast, solutions of the PC samples of concentrations greater than ~1% polymer displayed distinctly bimodal autocorrelation functions and relaxation time distributions. The onset of this bimodal behavior with increasing concentration corresponds to the onset of molecular overlap (c^*) and the peak in the total intensity vs. concentration profile. Figure 1 shows short- and long-time correlation functions for a semidilute solution of the 179 000 molecular weight PC sample. Shown also are the diffusion coefficient distributions for the two modes (only the fast-mode distribution is shown for the short-time correlation function; the CONTIN program cannot accurately determine the slow-mode distribution from the short-time correlation function data). Both of the two diffusive modes in these solutions are seen to have quite narrow distributions. Direct comparison of these distributions shows that the distribution of relaxation times in the slow mode is comparable in breadth to that for a dilute solution of monodisperse PMMA and narrower than for a dilute solution of polydisperse PMMA. The bimodal nature of the diffusive relaxation time distribution of the PC samples in semidilute solution was unaffected by a change in solvent ($CHCl_3$), elevation of the temperature (up to 66.6 °C), and length of time in solution (up to 1 year).

A careful determination was made of the characteristic diffusive relaxation times in each sample prepared. A study of the angular dependence of the relaxation rates indicated a linear dependence on q^2 (q is the scattering wavevector), affirming the diffusive nature of both the fast- and slow-mode relaxations. The fast-mode diffusion coefficients for several of the samples studied and the slow-mode diffusion coefficients for samples exhibiting this relaxation are plotted vs. concentration in Figure 2. The fast-mode diffusion coefficient is independent of molecular

Table I
Characteristics of the PMMA Samples

sample	M^a	$M_w/M_n{}^a$	source
PC-60	60 500	1.09	Pressure Chemical Co.
PC-125	125 000	1.08	Pressure Chemical Co.
PC-179	179 000	1.08	Pressure Chemical Co.
PC-240	240 000	1.09	Pressure Chemical Co.
PI-105	105 000	1.9	Polysciences, Inc.
PI-703	703 000	2.7	Polysciences, Inc.
PL-265	265 000	1.12	Polymer Laboratories, Ltd.
D-66[b]	66 000	1.4	DuPont
FR-200	~200 000	2	free radical polymerization, in situ, 40 °C

[a] M and M_w/M_n values reported by supplier except as follows: PI-105 and PI-703 values from our measurements using low-angle light scattering and GPC; FR-200 values predicted from kinetics. [b] D-66 sample was kindly provided by Dr. D. Y. Sogah of E. I. du Pont de Nemours and Co. Inc.

0024-9297/85/2218-0817$01.50/0

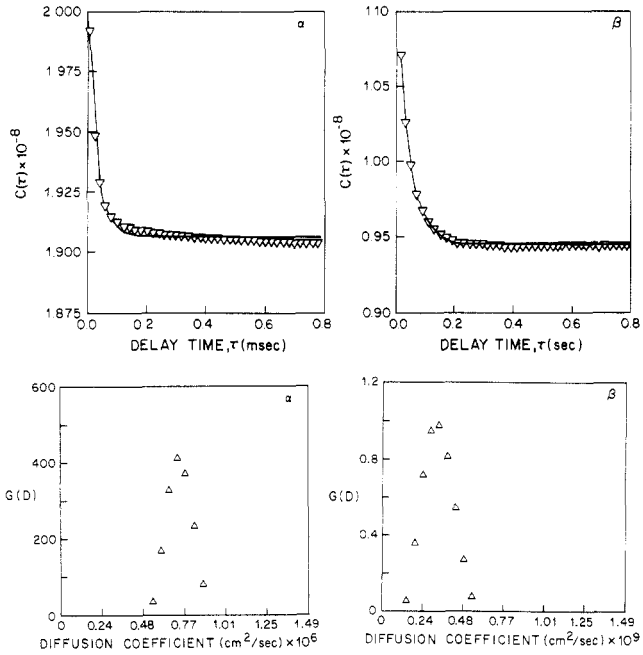

Figure 1. (Top) Autocorrelation function data for a 0.124 g/mL solution of sample PC-179 in MMA at 30 °C, $\theta = 60°$: (α) sample time $\Delta\tau = 10$ μs; (β) sample time $\Delta\tau = 10$ ms. The solid line represents a single-exponential fit to the data in both cases. Data points shown are for every second channel. (Bottom) Distribution of diffusion coefficients, $G(D)$, determined from the CONTIN program for the data presented above: (α) sample time $\Delta\tau = 10$ μs; (β) sample time $\Delta\tau = 10$ ms.

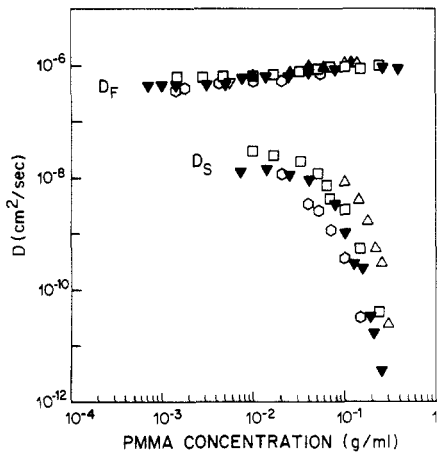

Figure 2. log–log plot of concentration dependence of the fast- and slow-mode diffusion coefficients for samples PC-60 (△), PC-125 (□), PC-179 (▼), PC-240 (○), and PI-105 (▲). Temperature = 30 °C.

weight above c^* as expected. The slow-mode diffusion coefficient is molecular weight dependent, varying as $1/M^2$, in agreement with the results of Amis and Han.[5] D_s falls off sharply with increasing concentration, in accord with previous findings on other polymer–solvent systems.[4-6] The slow-mode diffusion coefficient does not approach the self-diffusion coefficient at infinite dilution, which is given by the fast-mode coefficient.

The total scattered intensity of the 179 000 molecular weight PC sample has been measured over a wide range of concentrations and angles. Theoretically, osmotic effects lead to a peak in the intensity vs. concentration plot and a decaying intensity with increasing concentration beyond the peak.[14] This behavior is observed for light scattered from sample FR-200, which does not display a slow mode (see Figure 3). In contrast, the intensity of light scattered from the PC sample is anomalously high at higher concentrations. The source of the anomalous scattering can be discerned from the angular dependence of the scattered light. Characterization of the angular dependence allows determination of the radius of gyration of the scatterers.[11,15] With increasing concentration above c^*, the radius of gyration is found to increase dramatically (see Figure 4). Similar behavior was recently reported by Eisele and Burchard for the poly(vinylpyrrolidone)–water system.[11] Our preliminary results on the dependence of $\langle r_g^2 \rangle^{1/2}$ on concentration for the PI samples indicate that no similar size increase occurs. These results suggest that the clustering of polymer molecules into regions of higher than average density may be responsible for the unusual light scattering behavior observed for the PC samples. The dynamics of these transient clusters may lead to the slow mode.

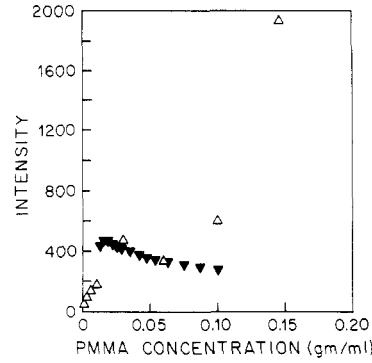

Figure 3. Total scattered intensity vs. concentration at $\theta = 60°$ for (▼) FR-200 and (△) PC-179.

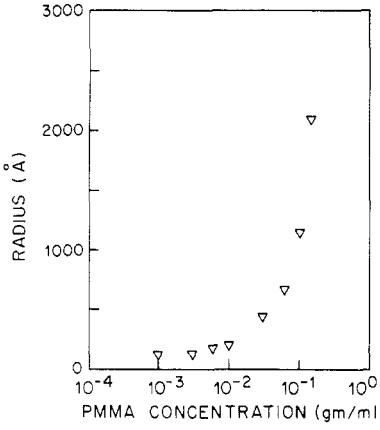

Figure 4. Radius of gyration (Å) vs. concentration for sample PC-179.

Analyses of the different PMMA samples are being conducted to determine which characteristics might lead to this clustering behavior. The NMR results for the PC and PI samples show them to have virtually identical tactic makeups. Similarly, the FTIR spectra of these samples show no apparent differences. Polydispersity is not a possible explanation as polydisperse blends of the PC samples also display a slow mode. Also, mixing of the PC and PI samples in semidilute solution in varying proportions yields a slow mode which gradually disappears as the amount of the PC sample is decreased to zero. Other approaches of sample analysis are under investigation.

On a more practical note, we have exploited the "different-yet-compatible" nature of the PC samples to undertake linear and network polymerization experiments using a PC sample as a wholly compatible tag species. This technique promises to provide insight into the effect of diffusion constraints on polymerization kinetics.

A more complete report of this work will appear elsewhere.

Acknowledgment. Use of the Sofica light scattering apparatus in the Department of Materials Science at Northwestern University through the good graces of Buckley Crist and John Torkelson is acknowledged with gratitude.

References and Notes

(1) T. Nose and B. Chu, *Macromolecules*, **12**, 590 (1979).
(2) B. Chu and T. Nose, *Macromolecules*, **12**, 599 (1979).
(3) B. Chu and T. Nose, *Macromolecules*, **13**, 122 (1980).
(4) E. J. Amis, P. A. Janmey, J. D. Ferry, and H. Yu, *Polym. Bull.*, **6**, 13 (1981).
(5) E. J. Amis and C. C. Han, *Polymer*, **23**, 1403 (1982).
(6) E. J. Amis, P. A. Janmey, J. D. Ferry, and H. Yu, *Macromolecules*, **16**, 441 (1983).
(7) W. Brown, R. M. Johnsen, and P. Stilbs, *Polym. Bull.*, **9**, 305 (1983).
(8) S. J. Candau, I. Butler, and T. A. King, *Polymer*, **24**, 1601 (1983).
(9) W. Brown, *Macromolecules*, **17**, 66 (1984).
(10) E. J. Amis, C. C. Han, and Y. Matsushita, *Polymer*, **25**, 650 (1984).
(11) M. Eisele and W. Burchard, *Macromolecules*, **17**, 1636 (1984).
(12) M. Adam and M. Delsanti, *Macromolecules*, **10**, 1229 (1977).
(13) S. W. Provencher, *Biophys. J.*, **16**, 27 (1976); S. W. Provencher, *Comput. Phys. Commun.*, **27**, 213 (1982).
(14) P. Debye and A. M. Bueche, *J. Chem. Phys.*, **18**, 1423 (1950).
(15) H. Benoit and M. Benmouna, *Polymer*, **25**, 1059 (1984).

Steven Balloge* and Matthew Tirrell

Department of Chemical Engineering and Materials Science, University of Minnesota Minneapolis, Minnesota 55455

Received December 4, 1984

Cellulose Crystallites: A Perspective from Solid-State ^{13}C NMR

In a solution, rapid molecular tumbling provides an averaged environment for each chemically distinct nucleus, resulting in an averaged chemical shift. In the solid-state, the molecules are constrained in the matrix and rapid molecular tumbling is no longer possible. Different molecular environments, be they due to inter- or intramolecular inequivalencies within the solid matrix, may give rise to multiple resonance lines for each nucleus. In the case of cellulose, while the solution ^{13}C NMR spectrum shows only six lines for the six carbons of the glucose residue,[1] the solid-state ^{13}C NMR spectra show additional lines. It has become evident that they are of two categories. The origin of each category, however, is a subject of continuous dialogue. The first category, which is apparent on C4 and C6, is manifested in a narrow and a broad component. These were initially assigned to different morphological sites.[2] Later studies[3,4] assigned them respectively to ordered and disordered regions. The most recent study[5] suggests that the narrow component arises from crystalline domains, and the broad component is associated with the surface of crystalline domains as well as with disordered regions. The present study will focus on the origin of the multiplets of the second category—those found on the narrow components of the first category.

In an early ^{13}C NMR study of solid cellulose conducted at 15.0 MHz,[6] doublets were observed for C1 in cellulose I and for C1 and C4 in cellulose II. Since C1 and C4 are the two carbons involved in the glycosidic linkages, these doublets were interpreted as reflecting two distinct glycosidic linkages within the same cellulose chain, i.e., a nonsymmetrical cellobiose-like repeat unit rather than a twofold helical conformation for successive glucose units. Dudley and co-workers[7] have recently come to a different conclusion. On the basis of NMR spectral analysis of a series of cellulose oligomers, they demonstrated that the observed doublets in cellulose II are due to two independent chains in the unit cell. This conclusion agrees well with the previous X-ray crystallographic studies,[8,9] which also show that cellulose II has a two-chain unit cell (see Figure 1) with the center chain staggered differently and of opposite polarity from the corner chains. In addition, the symmetry of the unit cell proposed from X-ray diffraction data is $P2_1$, and this symmetry precludes any equivalence between corner and center chains. Thus the observed doublets probably result from these two different crystallographic sites.

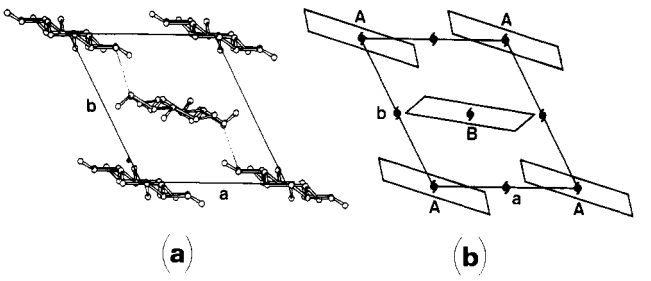

Figure 1. (a) Projection of cellulose II chains perpendicular to the *ab* plane along the fiber axis (courtesy of F. J. Kolpak[8]) and (b) schematic of the two-chain unit cell of cellulose II superimposed on a lattice with $P2_1$ symmetry.

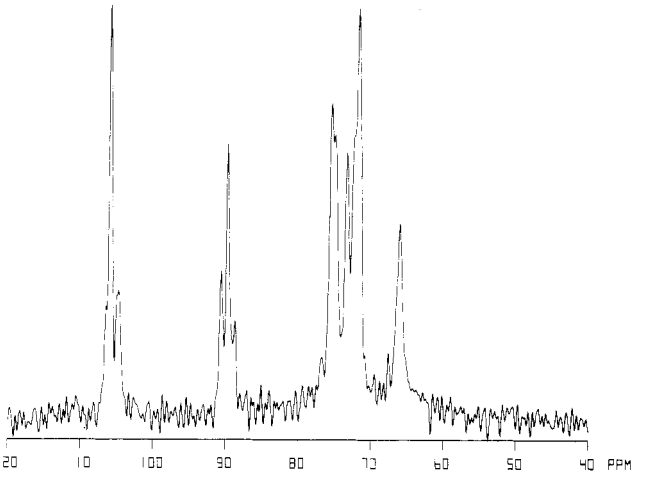

Figure 2. CP/MAS ^{13}C NMR spectrum of cellulose I (*Valonia macrophysa*), resolution enhanced.

In contrast to cellulose II, our 50.3-MHz spectrum of cellulose I (Figure 2) exhibits triplets for both C1 (105.7 ppm) and C4 (89.6 ppm). Earl and VanderHart[2] observed this same phenomenon earlier. In an attempt to reconcile this observation with an earlier study,[6] they suggested a unit cell containing four inequivalent glucose units with two different types of glycosidic linkages. We feel, however, that the origin of the observed triplets for cellulose I of *Valonia* and the doublets for cellulose II have a common basis, i.e., the symmetry and packing of chains in the unit cell. The absence of odd 00*l* reflections in the X-ray data[10,11] of crystalline cellulose indicates that any deviations from twofold screw symmetry must be very small. In addition, conformation analyses[12] favor cellulose chains possessing a conformation with or very close to a twofold screw symmetry. We note also that for most native celluloses, the 0-level (*hk*0) X-ray data can be indexed on a one-chain unit cell.[10,11] This implies that for cellulose I, the chain polarity is parallel and each chain has the same

0024-9297/85/2218-0819$01.50/0